New limit on the electron electric dipole moment

B. C. Regan,* Eugene D. Commins,† Christian J. Schmidt,‡ and David DeMille§
Physics Department, University of California, and Lawrence Berkeley National Laboratory, Berkeley, California 94720
(Dated: August 8, 2001)

We present the result of our most recent search for T-violation in ^{205}Tl, which is interpreted in terms of an electric dipole moment of the electron d_e. We find $d_e = (6.9 \pm 7.4) \times 10^{-28}\, e$ cm. The present apparatus is a major upgrade of the atomic beam magnetic-resonance device used to set the previous limit on d_e.

PACS numbers: 11.30.Er, 14.60.Cd, 32.10.Dk

We report a new result in the search for the electric dipole moment (EDM) of the electron, a quantity of interest in connection with CP violation and extensions to the standard model of particle physics [1–3]. In heavy paramagnetic atoms an electron EDM results in an atomic EDM enhanced by a factor $R \equiv d_{\rm atom}/d_e$. Thus we search for a permanent EDM of atomic thallium in the $6^2P_{1/2}\, F = 1$ ground state, where $R \simeq -585$ [4].

Experimental Method

Like its predecessor [5, 6], the new experiment [7] uses magnetic resonance with two oscillating rf fields [8] separated by a space containing an intense electric field **E**, and employs laser optical pumping for state selection and analysis. To control systematic effects arising from motional magnetic fields $\mathbf{E} \times \mathbf{v}/c$, the previous experiment employed a single pair of counterpropagating vertical atomic beams. The present experiment has two pairs separated by 2.54 cm, each consisting of Tl and Na (see Fig.1). The spatially separated beams are nominally exposed to identical magnetic but opposite electric fields; this provides common-mode noise rejection and control of some systematic effects. Sodium serves as a comagnetometer: it is susceptible to the same systematic effects but insensitive to d_e, since R is roughly proportional to the cube of the nuclear charge. Furthermore, sodium's two $3^2S_{1/2}$ ground state hyperfine levels F =2, 1 have $g_F = \pm 1/2$, which in principle permits the separation of two different types of motional field effects.

Figure 1 shows a schematic diagram of the experiment with the up beams active. Atoms leave the trichamber oven thermally distributed among the ground state hyperfine levels. After some collimation they enter the quantizing magnetic field **B**, nominally in the $\hat{\mathbf{z}}$ direction and typically 0.38 Gauss. Laser beams then depopulate the states with non-zero magnetic quantum numbers m_F. Thus, in the first optical region 590 nm $\hat{\mathbf{z}}$ polarized light selects the $m_F = 0$ Zeeman sublevel of either the $F = 2$ or the $F = 1$ Na ground state. In the second optical region 378 nm $\hat{\mathbf{z}}$ light selects the $m_F = 0$ sublevel of the Tl $F = 1$ ground state. The first rf region contains an oscillating magnetic field $\mathbf{B}_{\rm rf} = (B_{\rm Tl}\cos\omega_{\rm Tl}t + B_{\rm Na}\cos\omega_{\rm Na}t)\hat{\mathbf{x}}$, where $2B_{\rm Tl} = B_{\rm Na}$ and $1.506\omega_{\rm Tl} \simeq \omega_{\rm Na}$. These resonant fields apply '$\pi/2$' pulses, creating coherent superpositions of the $m_F \neq 0$ states of each species. The atoms then move into the electric field, nominally parallel or anti-parallel to **B**. Typically $|\mathbf{E}| = 1.23 \times 10^5$ V/cm. The second rf field is coherent with the first, differing only by a relative phase shift α. In the analysis regions the atoms are probed with the same laser that performed the state selection. Fluorescence photons accompanying the atomic decays are reflected by polished aluminum paraboloids into Winston cones[9] made of UV-transmitting plastic. These lightpipes are terminated by 1 cm^2 photodiodes.

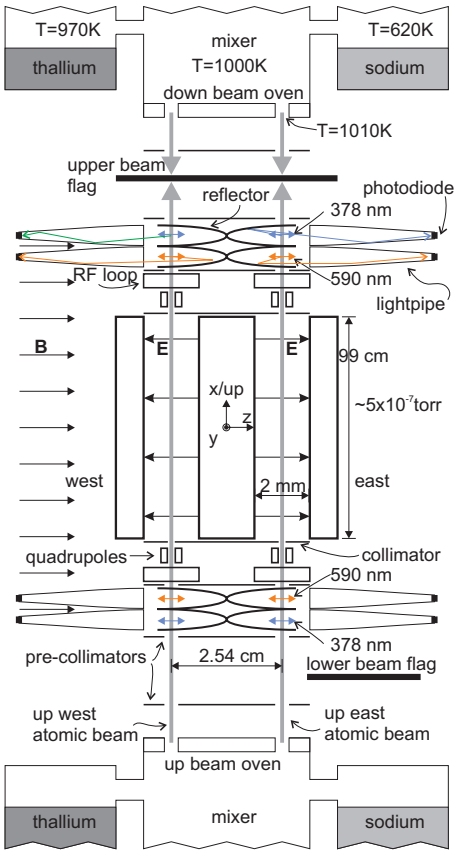

FIG. 1: Schematic depiction of the experiment, not to scale.

The resulting signals are approximated by the expression:

$$S \simeq \sum_{k=0}^{2F} < A_k \cos[k(\omega T - \int_0^T \gamma|B|dt - \varepsilon + \alpha)] > . \quad (1)$$

Here $< \ldots >$ means integration over the beam velocity distribution and trajectories. Also $\gamma = |g_F \mu_B|/\hbar$, T is the time of transit between the two rf regions, and :

$$\varepsilon \simeq \int_0^T \left[\frac{Rd_e}{\hbar}\frac{\mathbf{B}\cdot\mathbf{E}}{|\mathbf{B}|} + \frac{\gamma\mathbf{B}\cdot(\mathbf{E}\times\mathbf{v})}{|\mathbf{B}|c} + \frac{\gamma(\mathbf{E}\times\mathbf{v})^2}{2|\mathbf{B}|c^2} + \frac{\gamma\mathbf{B}\cdot\mathbf{B}_E}{|\mathbf{B}|}\right]dt + \frac{g_F}{|g_F|}\left[\frac{\mathbf{B}\cdot[\Delta\mathbf{B}\times(\mathbf{E}\times\mathbf{v})]}{c|\mathbf{B}|^3}\right]. \quad (2)$$

The first term, negligible for Na, arises from an EDM. The next two terms describe the $\mathbf{E}\times\mathbf{v}$ effect; the linear $\mathbf{E}\times\mathbf{v}$ term is largely cancelled by using the counter-propagating beams. Note that this term is strictly velocity-independent, since $\mathbf{v}dt = d\mathbf{r}$. The systematic error due to the quadratic $\mathbf{E}\times\mathbf{v}$ term is negligible, since it requires imperfect reversal of both $\mathbf{E}$ and $\mathbf{B}$. The fourth term describes the effect of a magnetic field $\mathbf{B}_E$ correlated with $\mathbf{E}$, such as might be generated by leakage and/or charging currents. The last term, odd in g_F, accounts for a geometric phase effect [10] that arises when the $\mathbf{E}\times\mathbf{v}$-induced motion of the quantizing axis couples to an unintended magnetic field change $\Delta\mathbf{B}$ between the entrance and exit of the electric field.

The coefficients A_k of eq. 1 describe how well $\mathbf{B}_{\rm rf}$ achieves the $\pi/2$-pulse condition. In addition, A_1 ($F = 1$) and A_1–A_3 ($F = 2$) depend upon quadratic corrections to the Zeeman splittings due to hyperfine mixing ($\propto \mathbf{B}^2$) and tensor Stark shifts ($\propto \mathbf{E}^2$). Thallium's large tensor Stark shift, 800 Hz at our E-field, makes this dependence a useful diagnostic tool.

In thallium the measurement proceeds as follows. After the optical and rf resonances have been located, the machine is cycled through 128 different configurations: 8 rf phases α [$\pm(90^\circ \pm 45^\circ \pm 1^\circ)$], 2 $\mathbf{E}$ polarities, 2 atomic beam directions, 2 high-voltage (HV) cable polarities, and 2 $\mathbf{B}$ polarities; see Fig. 2. (The associated full-periods are 75–150 ms for the rf, 3 s for $\mathbf{E}$, $\sim$ 1 min. for the beams, $\sim$ 1.5 hr for the cables and $\sim$ 3 hr for $\mathbf{B}$.) Since there are also east and west atomic beams, 256 independent linear combinations can be constructed. An EDM would manifest itself in the linear combination of signals that is odd, even, even, odd, even, odd, odd, and odd respectively. We obtain much diagnostic information from the other asymmetries. For instance, a $\pm45^\circ$-odd asymmetry shows the quadratic Stark effect, and a $\pm1^\circ$-odd asymmetry calibrates the sensitivity of the apparatus to phase shifts. For sodium the procedure is identical, with two exceptions: there are only 2 rf phase chops [$\pm(151^\circ \pm 1^\circ)$], since the quadratic Stark shifts are too small to be interesting; and there is the g_F reversal effected by employing either F state.

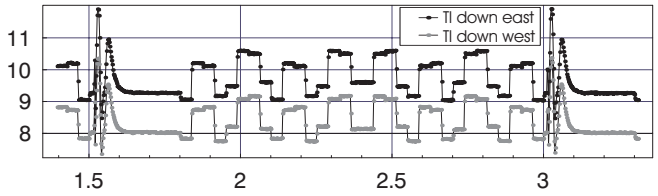

FIG. 2: This plot of typical raw data ($\dot{N}/10^8$ vs. t/s) shows two $\mathbf{E}$ switches and the intervening 32 rf phase chops. The decaying quadratic Stark shift oscillations give proof of a switching $\mathbf{E}$-field of the claimed magnitude.

Results

The EDM data consist of 44 sets obtained on six nights in the year 2000. (Despite careful shielding, environmental magnetic noise prevented data-taking during normal working hours.) Each set had 32-64 beam periods (bp), with $\sim$ 45 bp/set on average. The average current per detector was $\dot{N} \simeq 8.5 \times 10^8 e/s$. With a grand total of 1988 bp ($\sim$ 35 hrs) and a run-time duty cycle of 0.55, we collected $\simeq 5.2 \times 10^{13} e$ per up/down beam pair. Table I summarizes the raw results. The uncertainties are entirely statistical; in δ they are only 1.7 times the shot-noise limit. The noise in Σ is another 40% higher because of magnetic interference from the local electric train system BART[11].

Systematics: $\mathbf{E}\times\mathbf{v}$

Despite the excellent up/down beam cancellation, the motional field residuals are not negligible and require a correction. The EDM-like $\mathbf{E}\times\mathbf{v}$ systematic has the form

$$\varepsilon_{\mathbf{E}\times\mathbf{v}} \simeq \frac{g_F\mu_B}{2\hbar c}\int_{-L/2}^{L/2}(\Delta\mathbf{r}_{\rm ud}\cdot\nabla)\frac{\mathbf{B}\cdot(\mathbf{E}\times\mathbf{v})}{|\mathbf{B}|v_x}dx. \quad (3)$$

Since the atoms move in the x direction, the distance between the up and down beams $\Delta\mathbf{r}_{\rm ud}$ can only have y and z components. Allowing for x-even and x-odd versions brings the total number of displacement types to four, each of which couples to a different set of field gradients.

B	**C**	**Tl E**	**Tl W**	**Tl δ**	**Tl Σ**
even	even	-3.1±2.5	0.7±2.4	-1.3±1.4	-1.3±2.0
odd	even	2.2±2.5	3.2±2.4	-0.8±1.4	3.0±2.0
even	odd	1.8±2.5	-10.6±2.4	6.2±1.4	-4.2±2.0
odd	odd	8.8±2.5	8.4±2.4	-0.4±1.4	8.6±2.0

TABLE I: Raw EDM-like phases, in units of 10^{-7}. These are the linear combinations with respect to reversals of the magnetic field (**B**) and high voltage cables (**C**) of the uncorrected, **E**-odd, up/down-even phases. In addition to the values for the east and west beams, the east/west-odd (δ) and east/west-even (Σ) combinations are shown. An EDM would appear as a **B**-odd, **C**-odd δ. The **B**-even, **C**-odd effects are geometric phase residuals stemming from the $\Delta\mathbf{B}$ produced by the coils (*i.e.* the $\Delta\mathbf{B}$ that reverses with **B**), and do not contribute substantial systematic correction to the final result.

disp.	**dominant term**	**Tl East** $\varepsilon_{\rm cut}$	**Tl East** $\delta\nu_{\rm cut}$	**Tl West** $\varepsilon_{\rm cut}$	**Tl West** $\delta\nu_{\rm cut}$
δz	dE_y/dz	37±19	7.9	27±17	8.2
δv_z	(x-odd)	-45±11	8.7	14±13	8.5
δy	dBy/dy	-15±15	10.1	24±16	10.2
δv_y	(x-odd)	84±15	17.1	-113±19	16.6

TABLE II: $\mathbf{E}\times\mathbf{v}$ gradient summary. $\varepsilon_{\rm cut}$ is given in units of 10^{-7} and $\delta\nu_{\rm cut}$ in Hertz. The $\delta\nu$ are all assigned an uncertainty (systematic) of 0.1 Hz.

To control the $\mathbf{E}\times\mathbf{v}$ residuals we take EDM-type data with the atomic beams cut such that each of the four displacements is individually enhanced. We then apply gradients in B_z and measure rf resonance frequency differences $\delta\nu = \nu_{\rm up} - \nu_{\rm down}$ to determine these displacements. Similar measurements done during EDM data relate the spurious displacements to the enhanced ones. Then eq. 3 reduces to:

$$\varepsilon_{\mathbf{E}\times\mathbf{v}} = \sum_{\rm displacements} \varepsilon_{\rm cut}\frac{\delta\nu_{\rm uncut}}{\delta\nu_{\rm cut}}, \qquad (4)$$

which involves only measured quantities.

Table II summarizes [12] the measurements of ε with the atomic beams cut in half. The $\varepsilon_{\delta y}$ and $\varepsilon_{\delta z}$ were reduced by gradient-trimming prior to these measurements. Since the beams are not on the $z=0$ symmetry axis, an east/west-odd $\partial B_z/\partial z$ was present before the turn number ratio between two pairs of B_z coils at different $|z|$ positions was adjusted. Wedging of the center electrode relative to the outer ones by a small angle $\sim 2\times10^{-4}$ created a $\partial E_y/\partial z$. The quadrupoles electronically corrected this tiny mechanical imperfection, reducing the mean $\partial E_y/\partial z$ by 80%. They could also have corrected an x-odd $\partial E_y/\partial z$, had it been necessary.

Since the atomic beam slits could have clogged at any time, the relatively rapid measurements of $\delta\nu_{\rm uncut}$ were done twice each night. In all cases the average uncut displacements were less than 3% of the cut ones, implying that the ε's from Table II are suppressed by a factor of 30 or more in the real EDM data. For both beams the largest contribution to $\varepsilon_{\mathbf{E}\times\mathbf{v}}$ comes from the product of the x-odd δy ($\equiv \delta v_y$) and the x-odd $\partial B_y/\partial y$, which unfortunately was untrimmed. The mean $\mathbf{E}\times\mathbf{v}$ contributions to the measured phase total -0.2 ± 1.1 and -2.0 ± 1.2, in units of 10^{-7}, for the east and west beams respectively.

		$\lvert\mathbf{B}\rvert$ [mG]	ν [kHz]	scale	δ	Σ
low field						
10 July	Na	90	63.3	53.8	0.5±0.3	-0.4±0.5
15 Aug	Tl	90	42.0	18.1	1.1±0.2	0.7±0.4
23 Aug	Tl	60	27.9	41.0	-0.1±0.2	0.3±0.5
adopted	Tl	380	178.6	1.0	0.5±0.5	0.3±0.5

TABLE III: Low-field, **B**-odd, cable-odd effects scaled to their expected values for Tl at 179 kHz, assuming ε due to a geometric phase, in units of 10^{-7}. The sodium data reflect only the line-odd effect. These data were taken after a corrective gradient of $\partial B_x/\partial x \sim 10^{-6}$G/cm was applied.

Systematics: geometric phase

With large fluxes Tl and Na compete to leave the ovens. We generally favored thallium to sodium's detriment, limiting the utility of Na as a co-magnetometer. However, because the geometric phase effect $\varepsilon_{\rm geo}$ scales linearly with velocity, sodium is inherently three times more sensitive to $\varepsilon_{\rm geo}$, and it has the extra handle of g_F reversal. Thus we first studied $\varepsilon_{\rm geo}$ (by taking data at low values of **B**) with sodium. The data did not present a consistent picture. Detailed experimental, analytic and numerical follow-up investigations led to the discovery of a new type of systematic. Proportional to the product of a laser polarization misalignment and the non-adiabatic portion of the transition into or out of the electric field, this effect is **B**-even and substantial only in sodium at low field.

We thus decided to use thallium as well to look at the geometric phase. Table III shows data from both Na and Tl, scaled in accordance with the **B**-odd geometric phase hypothesis (assumes $\Delta\mathbf{B}$ due to a source other than the coils). The **B**-odd scaling $\sim v/B^2$ (see eq. 2) is fairly well supported in Σ, but the discrepancies in δ are significant. The values finally adopted for the geometric phase systematic contribution are the combination of the three sets of low field data shown. Because the agreement is unsatisfactory, we have enlarged the uncertainty sufficiently to make the three values consistent. Even though the east/west-odd ΔB_x is uncorrected, Σ here is comparable or smaller than δ, implying that the source of the non-reversing $\partial B_x/\partial x$ is distant from the atomic beams.

Systematics: charging and leakage currents

To place a limit on the size of leakage currents we charge the electric field plates to high voltage and then disconnect them from the supplies. After disconnection, decay of the electrode voltage is observed via the quadratic Stark shift asymmetry. Repeated measurements show a leakage current $\lesssim 2$ nA, with the probable current path remote from the atomic beams.

Charging currents are also determined by means of the Tl quadratic Stark effect, which is isolated by the rf chops alone. Thus there are four independent measurements of the electric field per **E**-switch. Binning the quadratic Stark asymmetry by time-after-**E**-chop shows a decaying charging current with an average value of 2 nA. Furthermore, binning the EDM asymmetry in the same way reveals no evidence of time dependence[13].

Dielectric absorption (DA) in the insulators that support the electrodes could lead to a current with a time constant $\gtrsim 1$ s and $\lesssim 1$ hr, which would evade the tests described already. Traditional electronic methods render this model implausible. Pathological quadrupole currents have been ruled out.

Totals

After correcting the raw data for the $\mathbf{E}\times\mathbf{v}$ and geometric phase effects, we have $\delta = -1.8\pm1.6$ and $\Sigma = 9.5\pm3.6$ (in units of 10^{-7}). See Tables IV and V. While there is no evidence of an EDM, the significant Σ indicates an as-yet-unexplained effect. Although we have considered many other possibilities, the best suspect is a $\mathbf{B}_E \sim 10^{-10}$G $\hat{\mathbf{z}}$. Given the electrode geometry, we require at minimum 10 nA to produce this $\mathbf{B}_E$, and such a large current is nearly excluded.

It is difficult to estimate how Σ affects the δ uncertainty. We have used various correlation analyses to limit, in a relatively model-independent way, the possible contamination of δ by Σ. The excessive, non-gaussian variability of Σ actually increases the power of this method. Assuming a worst-case $\mathbf{B}_E$ model (where a DA current in a single bad insulator located in the worst possible position produces $\delta/\Sigma \sim 1/6$) gives an equivalent total uncertainty, so we feel that this treatment is quite conservative. Most plausible $\mathbf{B}_E$ models give negligible δ/Σ.

Using $\bar{v} = 4.2\times10^4$ cm/s (measured two different ways), $R = -585$, and $E = 410$ statvolts/cm, we find that the final value for δ given in Table V implies $d_e = (6.9\pm7.4)\times10^{-28}e$ cm. The limit is $|d_e| \leq 1.6\times10^{-27}e$ cm with 90%-confidence.

We thank machinist A. Vaynberg and electronics engineer J. Davis for excellent work, and A. T. Nguyen, D. Budker, J. Clarke, Y. Zhang, and R. Falcone for useful discussions and assistance. We also gratefully acknowledge excellent work by the late machinists A. Brocato and S. Bonilla, and numerous technical contributions by the late Lars Commins. This work was supported by the Director, Office of Science, of the U.S. Department of Energy under Contract No. DE-AC03-76SF00098.

$\Sigma\,[10^{-7}]$					
date	$\lvert\mathbf{B}\rvert$[mG]	**raw**	$\mathbf{E}\times\mathbf{v}$	**geometric**	**total**
12-Jul	380	16.8±5.0	1.4±0.8	-0.27±0.5	17.9±5.1
13-Jul	"	2.7±5.1	2.0±0.9	"	4.4±5.2
15-Jul	"	1.9±4.3	0.8±0.7	"	2.4±4.4
12-Aug	"	1.6±4.8	0.6±0.7	"	1.9±4.9
30-Aug	"	10.3±5.9	1.5±0.8	"	11.5±6.0
24-Sep	760	19.7±4.6	0.4±0.8	-0.07±0.13	20.0±4.7
mean	-	8.6±2.0	1.1±0.8	-0.24±0.44	9.5±2.2

TABLE IV: Σ summary. This table shows the raw Σ data and corrections for each night. Because of the excessive variation in Σ from night to night, the value 2.2 for the total uncertainty is naive. A more realistic estimate is 3.6.

$\delta\,[10^{-7}]$				
date	**raw**	$\mathbf{E}\times\mathbf{v}$	**geometric**	**total**
12-Jul	-5.2±3.3	-1.2±0.8	-0.5±0.5	-6.9±3.4
13-Jul	-3.8±4.3	-0.6±0.9	"	-4.8±4.4
15-Jul	2.8±3.0	-1.4±0.7	"	0.9±3.1
12-Aug	-1.6±3.4	-0.6±0.7	"	-2.6±3.5
30-Aug	-0.3±3.4	-0.2±0.8	"	-1.0±3.5
24-Sep	3.5±3.3	-1.5±0.8	-0.12±0.13	1.8±3.4
mean	-0.4±1.4	-0.9±0.8	-0.43±0.46	-1.8±1.6
with Σ contribution to error				-1.8±1.9

TABLE V: δ summary. This table shows the raw δ data and corrections for each night.

* Electronic address: regan@physics.berkeley.edu
† Electronic address: commins@physics.berkeley.edu
‡ Electronic address: christian.j.schmidt@de.abb.com
§ Electronic address: david.demille@yale.edu

[1] I. B. Khriplovich and S. K. Lamoreaux, *CP Violation Without Strangeness: Electric Dipole Moments of Particles, Atoms, and Molecules* (Springer, New York, 1997).
[2] E. D. Commins, Am. J. Phys. **61**, 778 (1993).
[3] E. D. Commins, in *Advances in Atomic, Molecular, and Optical Physics* (Academic Press, 1999), vol. 40, pp. 1–55.
[4] Z. W. Liu and H. P. Kelly, Phys. Rev. A **45**, R4210 (1992).
[5] K. Abdullah, C. Carlberg, E. D. Commins, H. Gould, and S. B. Ross, Phys. Rev. Lett. **65**, 2347 (1990).
[6] E. D. Commins, S. B. Ross, D. DeMille, and B. C. Regan, Phys. Rev. A **50**, 2960 (1994).
[7] B. C. Regan, Ph.D. thesis, University of California, Berkeley, Physics Department (2001), available from the

author or http://www.umi.com.
[8] N. F. Ramsey, *Molecular Beams* (Oxford University Press, London, 1956), chapter V., Sec. 4 and references therein.
[9] W. T. Welford and R. Winston, *High Collection Nonimaging Optics* (Academic Press, San Diego, 1989).
[10] E. D. Commins, Am. J. Phys. **59**, 1077 (1991).
[11] A. C. Fraser-Smith and D. B. Coates, Radio Science **13**, 661 (1978).
[12] 'Summarize' in this case means the displacement-odd, **B**-odd, and cable-odd component; the other linear combinations are generally not significant.
[13] This point also argues against any effect caused by the shields, which are observed to have a 70 ms time constant.